CRYSTAL GROWTH & DESIGN

Article

pubs.acs.org/crystal

Rigidity versus Flexibility of Ligands in the Assembly of Entangled Coordination Polymers Based on Bi- and Tetra Carboxylates and N-Donor Ligands

Shu-Long Wang,[†,‡,#] Fei-Long Hu,[†,§,#] Ju-Ying Zhou,[‡] Yan Zhou,[‡] Qin Huang,*[,‡] and Jian-Ping Lang*[,†]

[†]College of Chemistry, Chemical Engineering and Materials Science, Soochow University, Suzhou 215123, P. R. China

[‡]Guangxi Key Laboratory of Chemistry and Engineering of Forest Products, Guangxi University for Nationalities, Nanning, 530006, P. R. China

[§]Guangxi Colleges and Universities Program of Innovative Research Team and Outstanding Talent, College of Chemistry and Material, Yulin Normal University, Yulin, 537000, P. R. China

S *Supporting Information*

ABSTRACT: Seven Zn(II) coordination polymers including [Zn(pbda)(*p*-bimb)]·H_2O (**1**), [Zn(pbda)$(bpa)_{0.5}$] (**2**), [Zn(pbda)(bpp)] (**3**), [$Zn(Hpbda)_2(bibm)_2$] (**4**), [$Zn(pbta)_{0.5}$(m-bimb)]·H_2O (**5**), [$Zn(pbta)_{0.5}$(bpp)(H_2O)] (**6**), and [$Zn(H_2pbta)$(bibm)]·H_2O (**7**) (H_2pbda = 4,4′-{[1,4-phenylenebis(methylene)]bis(oxy)}dibenzoic acid; p-bimb = 1,4-bis(1*H*-imidazol-l-yl)methyl)benzene; bpa = 1,2-bis(4-pyridyl)ethane; bpp = 1,3-bis(4-pyridyl)-propane; bibm = 4,4′-di(1*H*-imidazol-1-yl)-1,1′-biphenyl; m-bimb = 1,3-bis(1*H*-imidazol-l-yl)methyl)-benzene; H_4pbta = 5,5′-phenylenebis(methylene)-1,1′-3,3′-(benzene-tetracarboxylic acid) were prepared under solvothermal conditions and structurally characterized. Compound **1** shows a three-dimensional (3D) channel-like architecture constructed by helical chain subunits. Compound **2** shows a rare 2D + 2D + 2D → 2D network with both polyrotaxane and polycatenane features. **3** holds a 2D layer structure constituted of metal-sharing right- and left-handed helical chains. Compound **4** presents a one-dimensional (1D) chain which is decorated by long side arms around the chain. Compound **5** possesses a 2D wave-like layer formed by [Zn_2(*m*-bimb)]$_n$ chains by linear pbta ligands. Compound **6** displays a 3D framework that is stabilized by hydrogen bonding interactions between the coordinated H_2O molecules and the neighboring carboxylate oxygen atoms. Compound **7** possesses a 1D + 1D → 2D polycatenation motif. The results demonstrated that the rigidity versus flexibility of the ligands along with the number of carboxyl groups make an impact on the structural diversities of the entangled coordination polymers. Moreover, compounds **3** and **6** as representative examples possessed high catalytic efficiency for the photodecomposition of methyl blue in water using natural sunlight irradiation.

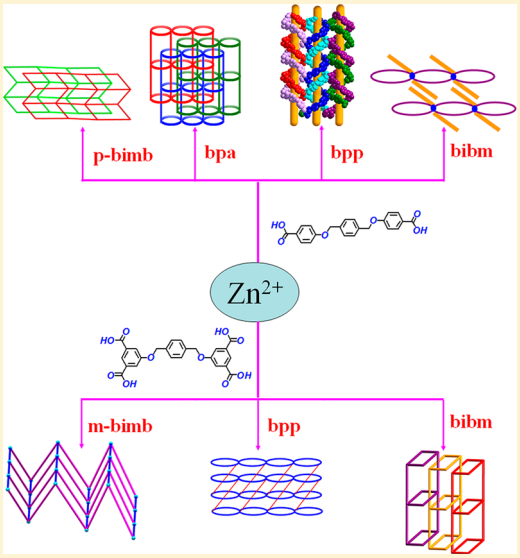

INTRODUCTION

Design and synthesis of novel entangled networks have attracted great attention due to their interesting topological architectures and potential applications.[1−9] It is still difficult to identify the main factors directing the final structures[10−12] because many factors such as auxiliary ligands,[13,14] metal ions,[15] reaction temperatures,[16] pH values,[17] etc. may affect the diversities of the resulting assemblies.[18−21] It is well-known that the design and selection of suitable ligands are quite critical in the formation of the coordination frameworks. The rigidity and flexibility of the ligand employed should be specially considered.[22−31] Therefore, the appropriate organic ligands along with the careful control of reaction conditions are key factors for achieving entangled coordination polymers (CPs).

Polycarboxylate ligands may have many kinds of coordination modes and have been extensively adopted in the preparation of CPs. In the family of polycarboxylate ligands, biphenyl-based bi- and tetracarboxylates are of special interest because the two phenyl rings can freely rotate to generate different conformations.[32] If the two phenyl groups of the ligand are separated by other groups such as −O−, −CH_2−, and −O−CH_2−, the phenyl groups may freely rotate around these groups according to the coordination requirement of the metal ions in the assembly process. Moreover, the carboxylate arms can readily change their conformations to satisfy the

Received: May 18, 2015
Revised: June 20, 2015

DOI: 10.1021/acs.cgd.5b00642
Cryst. Growth Des. XXXX, XXX, XXX−XXX

Scheme 1. Structures of H_2pbda and H_4pbta and Auxiliary N-Donor Ligands Used in This Work

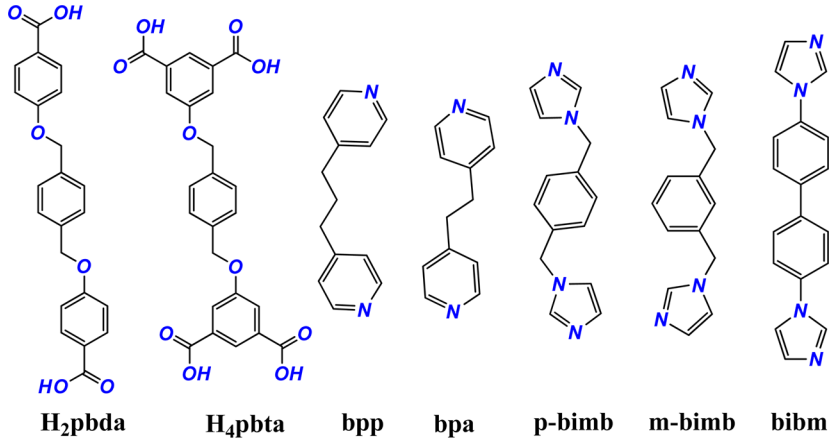

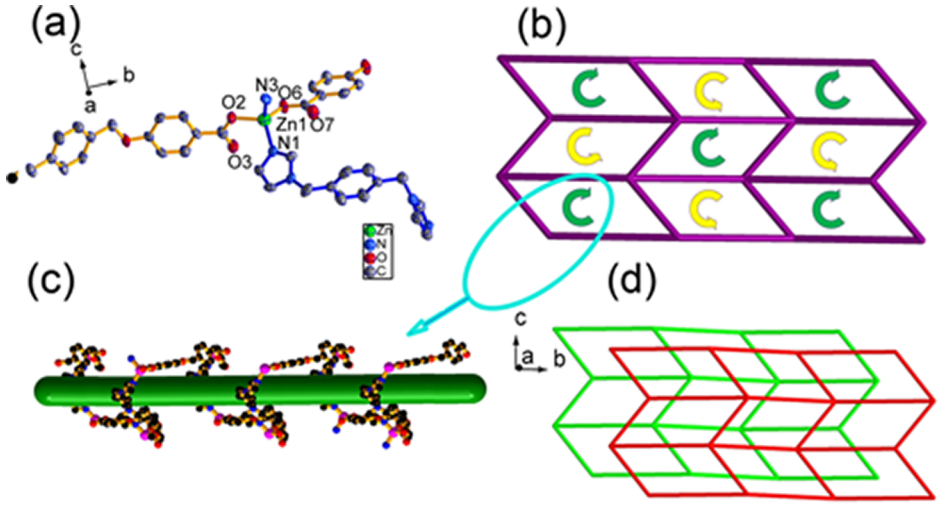

Figure 1. (a) View of the coordination environment of the Zn(II) center in **1**. (b) View of the helical channels in the 3D architecture of **1**. (c) View of a section of the 1D meso-helical chain. (d) The simplified representation of the 2-fold interpenetration in **1**.

coordination requirements of the metal ions through their "breathing" behavior in the solid state.[33] On the contrary, if two or more carboxyl groups on the same phenyl ring coordinate to one metal ion, the phenyl ring is fixed and turned rigid to some extent. Therefore, the tetracarboxylate ligands separated by $-O-CH_2-$phenyl$-CH_2-O-$ groups are expected to show both flexible and rigid properties in the assembly of CPs.

On the other hand, the N-donor ligands also have a crucial influence in the assembly process.[34−45] Up to now, a large number of CPs containing flexible or rigid N-donor ligands have been reported.[46−50] The rigid one possesses a certain rigidity and stability, which can reduce the uncertainty in the assembly process. However, the flexible N-donor ligands may take different coordination modes, which increase the complexity of the resulting coordination polymers.

In this article, we designed and synthesized two poly(carboxylic acid) ligands, 4,4′-{[1,4-phenylenebis(methylene)]-bis(oxy)}dibenzoic acid (H_2pbda)[51] and 5,5′-phenylenebis-(methylene)-1,1′-3,3′-(benzene-tetracarboxylic acid)[52] (H_4pbta) (Scheme 1). Their reactions with $ZnSO_4$ in the presence of five auxiliary N-donor ligands (Scheme 1) (1,4-bis(1*H*-imidazol-l-yl)methyl)benzene (p-bimb); 1,2-bis(4-pyridyl)ethane (bpa); 1,3-bis(4-pyridyl)-propane (bpp); 4,4′-di(1*H*-imidazol-1-yl)-1,1′-biphenyl (bibm); 1,3-bis(1*H*-imidazol-l-yl)methyl)-benzene (m-bimb)) under solvothermal conditions produced seven coordination polymers: [Zn(pbda)(p-bimb)]·H_2O (**1**), [Zn(pbda)(bpa)$_{0.5}$] (**2**), [Zn(pbda)(bpp)] (**3**), [Zn(Hpbda)$_2$(bibm)$_2$] (**4**), [Zn(pbta)$_{0.5}$(m-bimb)]·H_2O (**5**), [Zn(pbta)$_{0.5}$(bpp)(H_2O)] (**6**) and [Zn(H_2pbta)(bibm)]·H_2O (**7**). All these compounds were characterized and structurally determined. The effects of rigidity versus flexibility of ligands employed on the structural diversities of these compounds are discussed. In addition, compounds **3** and **6** were selected as representative examples and presented good photocatalytic performances in decomposing methyl blue (MB) in water under sunlight.

RESULTS AND DISCUSSION

Synthesis and Characterization. The reactions of $ZnSO_4$·$7H_2O$ with H_2pbda and p-bimb (molar ratio = 2:1:1) in H_2O/DMF (v/v = 6:4) at 145 °C for 2 days under solvothermal conditions gave colorless crystals of **1** in 52% yield. Other similar reactions of $ZnSO_4$·$7H_2O$ with H_2pbda and L (molar ratio = 2:1:1) or $ZnSO_4$·$7H_2O$ with H_4pbta and L afforded colorless crystals of **2** (60% yield) for L = bpa, **3** (40% yield) for L = bpp, and **4** (45% yield) for L = bibm, block crystals of **5** (50% yield) for L = m-bimb, block crystals of **6** (60% yield) for L = bpp, and sheet crystals of **7** (48% yield) for L = bibm, respectively. In addition, analogous reaction of $ZnSO_4$·$7H_2O$

DOI: 10.1021/acs.cgd.5b00642
Cryst. Growth Des. XXXX, XXX, XXX−XXX

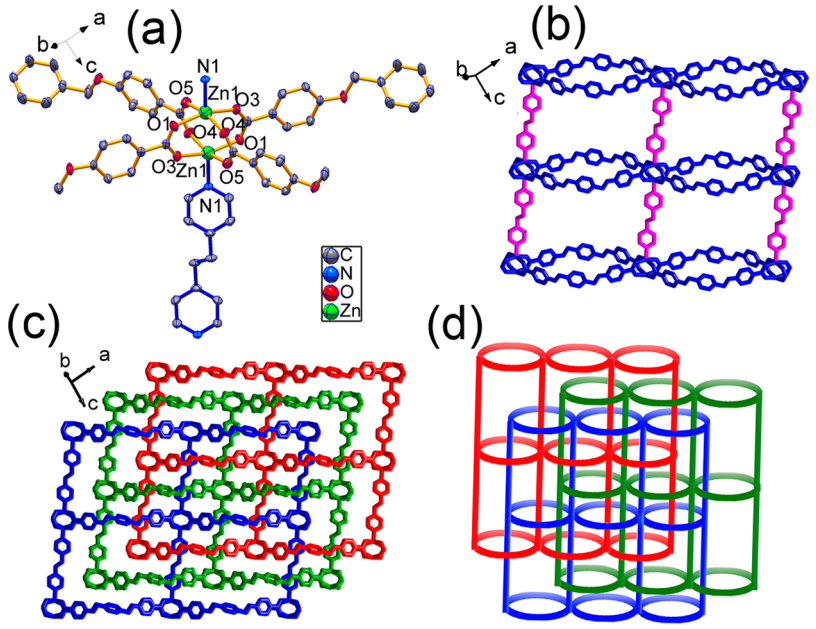

Figure 2. (a) View of the coordination environment of the Zn(II) center in **2**. (b) View of the single 2D sheet in **2**. (c) View of three interpenetrating sheets in **2**. (d) Schematic view of the parallel 2D → 2D 3-fold interpenetration in **2**.

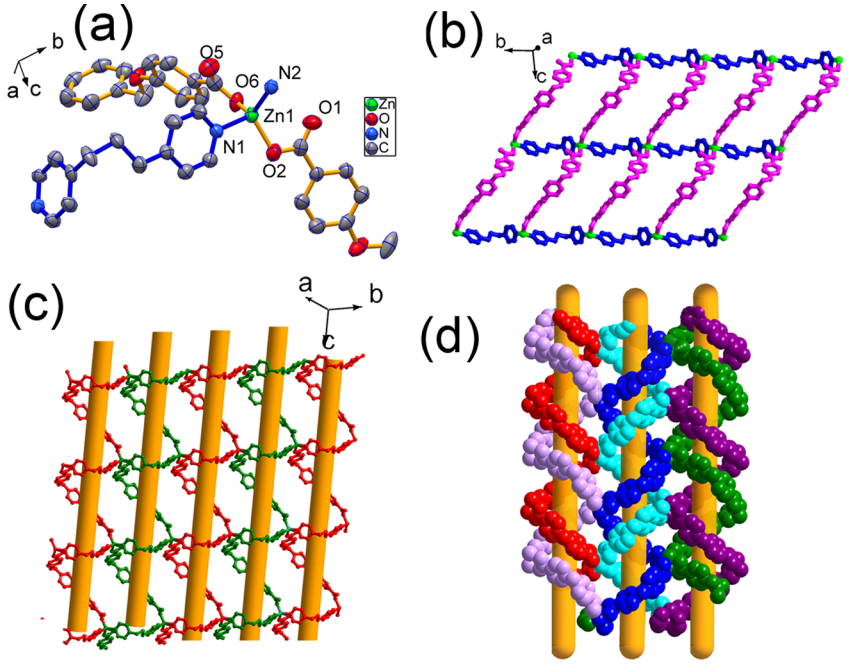

Figure 3. (a) View of the coordination environment of the Zn(II) center in **3**. (b) View of the single 2D layer in **3**. (c) View of the 2D layer constituted by helical chains in **3**. (d) Two identical layers interpenetrated into each other forming the 2D + 2D → 2D in **3**.

with H_4pbta and bpa afforded colorless crystals of a known compound $[Zn_2(pbta)(bpa)_2]\cdot 4H_2O$.[14] Compounds **1**−**7** are air-stable and do not dissolve in water and other organic solvents. The observed C, H, and N contents of **1**−**7** matched well with their theoretical ones. The experimental powder X-ray diffraction (PXRD) patterns of **1**−**7**, measured at room temperature, were consistent with the simulated ones, suggesting the good phase purity of these compounds (Figures S1 and S2). The IR spectra of **1**−**7** exhibited asymmetry and symmetric stretching vibrations of the coordinated carboxylate groups at 1521−1634 cm^{-1} and 1321−1489 cm^{-1}.[53−58] The ν_{as}(COOH) of the uncoordinated carboxyl group in **7** appeared at 1706 cm^{-1}. The ν(O−H) of the coordinated and lattice water molecules in **1** and **5**−**7** were located in the range of 3100 and 3500 cm^{-1}.[54] The bands of 1540−1622 cm^{-1} in **1**, **4**, **5**, and **7** referred to the C═N stretching vibration of imidazole rings.[55,58,59]

Crystal Structure of [Zn(pbda)(p-bimb)]·H_2O (1). Compound **1** belongs to the $P2_1/c$ space group, and its asymmetric unit consists of one [Zn(pbda)(p-bimb)] unit and one solvent water molecule. Each Zn(II) atom is tetrahedrally coordinated by two O atoms from two pbda ligands and two N atoms from two p-bimb ligands (Figure 1a). In **1**, each p-bimb links two Zn(II) centers to afford a $[Zn_2$(p-bimb)] unit that

DOI: 10.1021/acs.cgd.5b00642
Cryst. Growth Des. XXXX, XXX, XXX−XXX

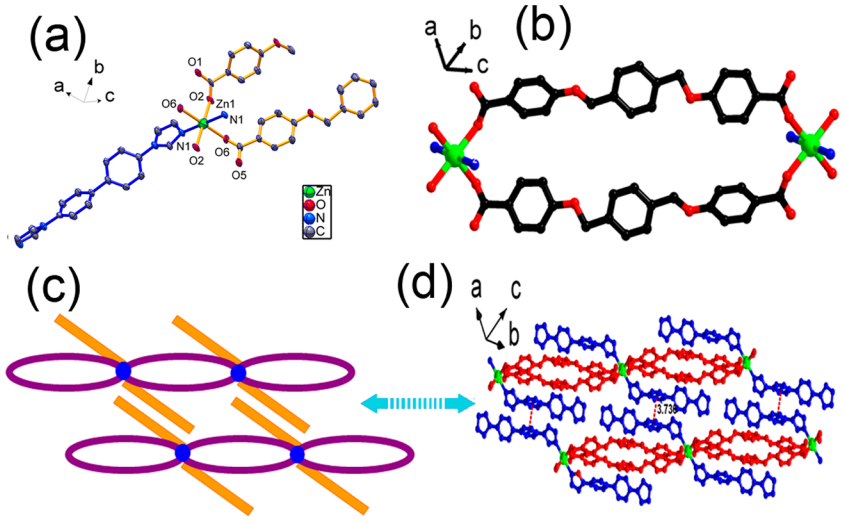

Figure 4. (a) View of the coordination environment of the Zn(II) center in **4**. (b) View of the $[Zn_2(pbda)_2]$ unit. (c) Schematic description of the $\pi\cdots\pi$ stacking interactions of **4**. (d) Viewing of the 2D supramolecular layer formed by $\pi\cdots\pi$ stacking interactions between the benzene of bibm ligands in **4**.

propagates into a 1D chain along the *c* axis. Two adjacent chains are interconnected by pbda ligands into a railway-like motif. Half of one pbda ligand links the $[Zn_2(p\text{-}bimb)]_n$ chains along the parallel direction, while the other half hooks the two adjacent $[Zn_2(p\text{-}bimb)]_n$ chains in a up-and-down way. A three-dimensional (3D) framework with a one-dimensional (1D) helical channels along the *a* axis is thus observed in **1** (Figure 1b,c). Such a structure could be simplified as a 3D + 3D → 3D interpenetrated net (Figure 1d). The C−H···π and hydrogen bonding interactions play significant roles in the stabilization of the 3D framework of **1** with a C(35)−H(35)···Cg distance of 2.93(7) Å (Cg is the center of benzene ring constituted by C(2) to C(7)). In **1**, each pbda displays a linear linker in which two benzoates slightly rotate around the −O− or $-O-CH_2-$ units, while the two imidazole rings of p-bimb do much around these units to satisfy the requirement of the Zn(II) coordination geometry.

Crystal Structure of $[Zn(pbda)(bpa)_{0.5}]$ (2). Compound **2** belongs to the $P\bar{1}$ space group, and its asymmetric unit has one $[Zn(pbda)(bpa)_{0.5}]$ unit. Each Zn(II) center adopts a distorted square pyramidal geometry, coordinated by four O atoms from four H_2pbda ligands and one N atom from bpa (Figure 2a). A paddled-wheel $[Zn_2(COO)_4]$ subunit with four carboxyl groups of pbda ligand chelating two Zn(II) centers is formed with a short Zn···Zn distance of 2.909 Å. Two pbda ligands link two $[Zn_2(COO)_4]$ subunits to yield an elliptic $[Zn_4(pbda)_2]$ unit. Such units expand along the (−101) direction through bpa ligands to generate a two-dimensional (2D) network[60−62] (Figure 2b). Three identical 2D networks interpenetrate into each other in a 2D + 2D + 2D → 2D parallel fashion, thereby forming an uncommon 2D polyrotaxane layer (Figure 2c). In this way, bpa acts as a rod to pass through the loop of the $[Zn_4(pbda)_2]$ unit and vice versa (Figure 2d). Adjacent layers are stacked together through C−H···π and lone pair···π interactions (O(6)···Ch = 3.57(9) Å, C(8)−H(8)···Ci = 2.82(2) Å; Ch is center of phenyl group constituted by C(16) to C(21); Ci is the center of ring defined by C(2) to C(7)). To our knowledge, such a 2D entanglement sheet that exhibits both polyrotaxane and polycatenane features is quite rare.[21,63−65]

Crystal Structure of [Zn(pbda)(bpp)] (3). Compound **3** belongs to the $P\bar{1}$ space group, and its asymmetric unit consists of one discrete [Zn(pbda)(bpp)] unit. Each Zn(II) center is tetrahedrally coordinated by two O atoms from two pbda molecules and two N atoms from two bpp molecules (Figure 3a). Three phenyl rings of each pbda are noncoplanar and rotate away with dihedral angles of 63.4(5)° and 61.4(6)° between the central phenyl and the adjacent ones. Each pbda or bpp ligand links two Zn(II) centers, while each Zn(II) binds four pbda or bpp ligands to afford a 2D layer (Figure 3b). Analysis of the packing of **3** reveals that the layer is assembled through the rhombus ring with side lengths of 11.616 Å × 18.424 Å. Pbda and bpp ligands alternatively bridge Zn(II) centers to form left- and right-handed helical chains extending along the *c* axes, where the right- and left-handed helices are formed equally with the pitch of 15.685 Å. As shown in Figure 3c, adjacent helical chains are joined together by Zn(II)-sharing, thereby forming an achiral 2D layer. Two identical layers interpenetrate each other into a 2D + 2D → 2D fashion (Figure 3d). Neighboring layers are further stacked into a 3D structure through the edge-to-face interactions and strong hydrogen bonds.

Crystal Structure of $[Zn(Hpbda)_2(bibm)_2]$ (4). Compound **4** conforms to the $P\bar{1}$ space group, and its asymmetric unit has one $[Zn(Hpbda)_2(bibm)_2]$ unit. The Zn(II) center is octahedrally coordinated by two N atoms from two bibm ligands and four carboxyl O atoms from four pbda ligands (Figure 4a). One carboxyl group of the pbda ligand in **4** is protonated in order to balance the negative charge. The bond lengths of Zn−O vary in the range of 2.216(3)−2.239(4) Å, and the Zn−N bond length of 2.202(4) Å is normal according to the literature.[66] Two Zn(II) centers are joined by two $Hpbda^-$ ligands to form a $[Zn_2(Hpbda)_2]$ subunit, which propagates along the *c* axis into a 1D chain (Figure 4b). The bibm ligands decorate the chain on both left and right sides with one of two iminazole groups being intact. The neighboring chains are connected by $\pi\cdots\pi$ stacking interactions with a distance of 3.736 Å between two aromatic rings (Figure 4c,d). Because of the absence of the flexibility, the rigid bibm cannot rotate its uncoordinated iminazole group to meet the Zn coordination.

DOI: 10.1021/acs.cgd.5b00642
Cryst. Growth Des. XXXX, XXX, XXX−XXX

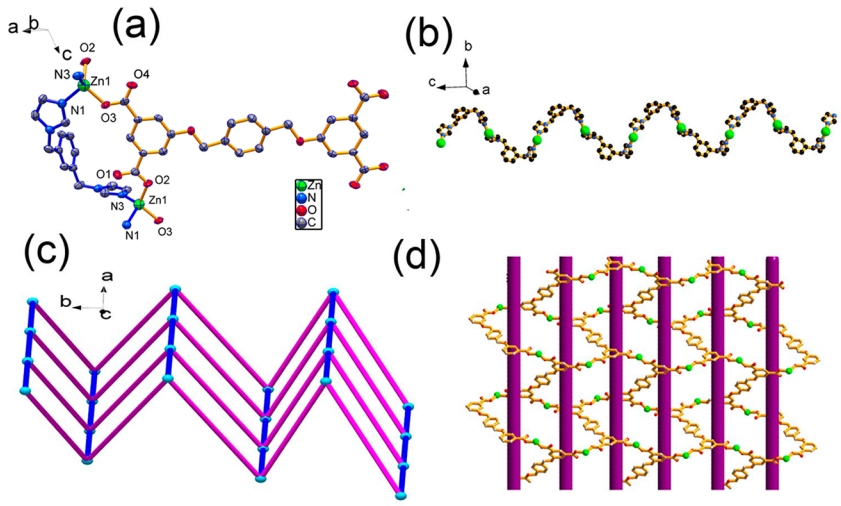

Figure 5. (a) View of the coordination environment of the Zn(II) center in **5**. (b) View of a portion of the 1D helical $[Zn(m\text{-}bimb)]_n$ chain (c) Schematic representation of a ***sql*** net of **5**. (d) View of the 1D helical channels in **5**.

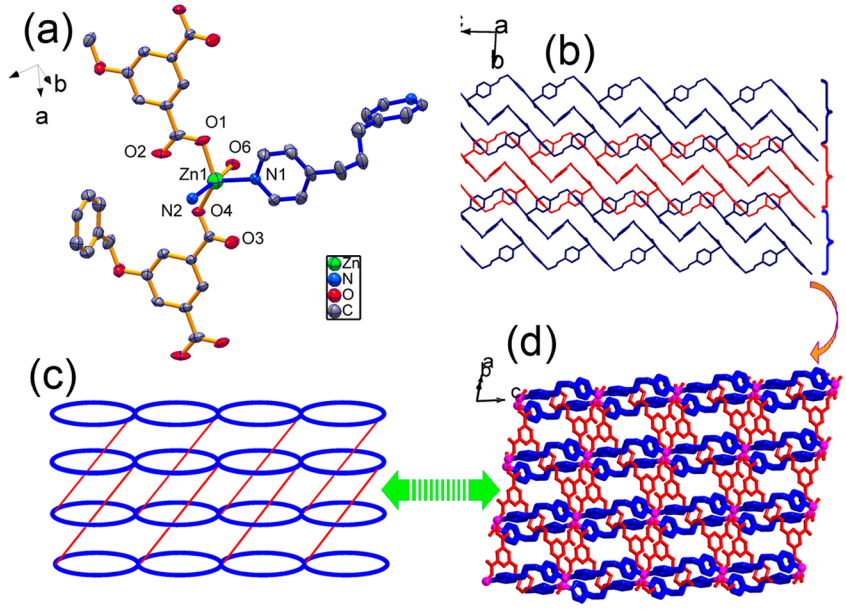

Figure 6. (a) View of the coordination environment of the Zn(II) center in **6**. (b) View of the 1D + 1D → 3D polycatenation in **6**. (c) Schematic view of the interpenetrating nets of **6**. (d) View of the 3D interpenetrating structure of **6**.

Crystal Structure of $[Zn(pbta)_{0.5}(m\text{-}bimb)]\cdot H_2O$ (5). Compound **5** conforms to the $P2_1/c$ space group, and one $[Zn(pbta)_{0.5}(m\text{-}bimb)]$ unit and one water solvent molecule are contained in its asymmetric unit. Each Zn(II) center is tetrahedrally coordinated by two N atoms from m-bimb and two O atoms from pbta ligands (Figure 5a). The average bond lengths of Zn−O (1.951(3) Å) and Zn−N (2.029(4) Å) are comparable to the corresponding value in **1**. Each m-bimb in **5** bridges two Zn(II) centers to generate a $[Zn_2(m\text{-}bimb)]$ unit, which propagates along the *c* axis to yield a $[Zn_2(m\text{-}bimb)]_n$ chain (Figure 5b). The $[Zn_2(m\text{-}bimb)]_n$ chains are interconnected by linear pbta ligands to form a ***sql*** layer (Figure 5c). Compared with the flexibility of m-bimb, the three phenyl rings in each pbta are nearly coplanar with the dihedral angles of 10.54°, indicating the approximate rigidity of pbta. The 1D helical channels are formed by cross-linked pbta ligands along the *b* axis (Figure 5d). The 2D layers are further developed into a 3D structure by hydrogen bonds and $\pi\cdots\pi$ stacking interactions with the center-to-center distance of 3.978 Å (Cj···Cj′ = 3.978 Å, Cj is the benzene ring constituted by C16 to C21, while Cj′ is the center of benzene ring constituted by C24, C25, C26, and their equivalents).

Crystal Structure of $[Zn(pbta)_{0.5}(bpp)(H_2O)]$ (6). Compound **6** belongs to the $P\bar{1}$ space group, and its asymmetric unit has one $[Zn(pbta)_{0.5}(bpp)(H_2O)]$ unit. Each Zn(II) center adopts a trigonal bipyramidal geometry, coordinated by two N atoms from bpp and three O atoms from pbta and water molecule, respectively. The average bond length of Zn−O (2.063(3) Å) is longer than that found in $[Zn(bdc)(4,4'\text{-bipy})(H_2O)]\cdot 1.5H_2O$ (1.952(2) Å, bdc = 1,3-benzenedicarboxylates, 4,4′-bipy = 4,4′- bipyridine),[67] while the mean Zn−O(H_2O) and Zn−N (2.173(3) vs 2.093(3) Å) bond lengths are shorter than those observed in $[Zn(bdc)(4,4'\text{-bipy})(H_2O)]\cdot 1.5H_2O$ (2.167(2) Å vs 2.188(2) Å). As shown in Figure 6b, a zigzag chain along the *c* axis is formed through the linkage of bpp and Zn centers. Two adjacent chains are joined by two

DOI: 10.1021/acs.cgd.5b00642
Cryst. Growth Des. XXXX, XXX, XXX−XXX

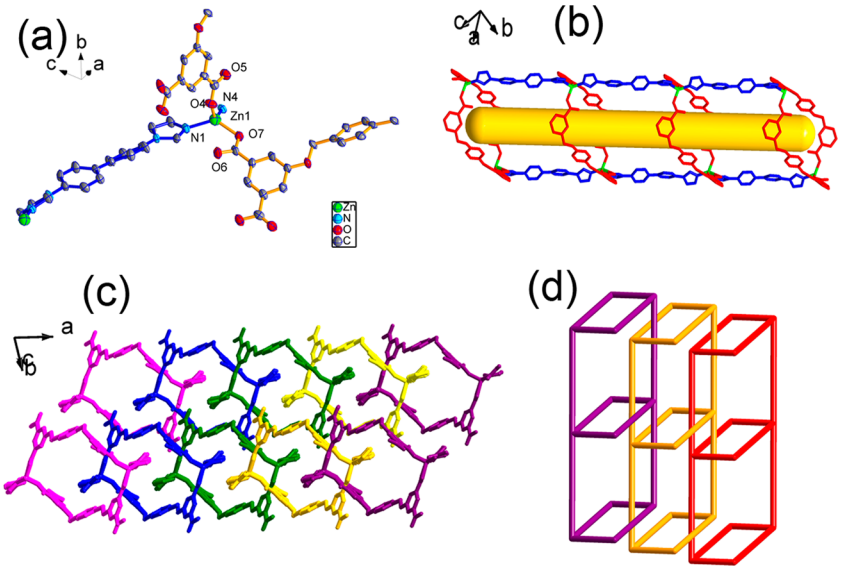

Figure 7. (a) View of the coordination environment of the Zn(II) center in **7**. (b) View of one section of the 1D rectangle-shaped nanotube of **7**. (c) View of the 1D + 1D → 2D polycatenation in **7**. (d) Schematic presentation of the 3-fold interpenetration in **7**.

carboxyl groups from each pbta to give a railway-like double chain. Such chains propagate along the *ac* plane to form a 2D layer structure by the connection of the remaining carboxyl groups of the pbta ligands with Zn centers. The adjacent layers are further stacked into a 3D framework by C−H···π (C−H···Cg = 2.958 Å, C−H···Cg = 154.4°, Cg is the center of the pyridine ring constituted by N2, C1 to C5) and hydrogen bonding (O6−H−O2, O6−H−O4) interactions. Each pbta displays a "Z-shaped" motif with a dihedral angle of 82.9(8)° between the central and terminal phenyl rings. Unlike **5**, in which each pbta shows a linear pattern, the pbta ligand in **6** encapsulates the space decorated by the $[Zn_n(bpp)_m]$ units and function as pillars to support the $[Zn_n(bpp)_m]$ units (Figure 6c,d). The two pyridine rings of the bpp ligands in **3** and **6** are arranged in a nearly parallel fashion (82.98° vs. 89.6°). However, **3** and **6** present completely different networks due to the different carboxylate ligands used. The dihedral angle of two pyridyl rings located at the axial direction is 103°, implying that two pyridyl rings bend seriously along the $-CH_2-CH_2-CH_2-$ group. This may ascribed to the requirement of the arched conformation of pbta. This structural information suggests that pbta and bpp in **6** serve as flexible ligands. It seems that bpp is more flexible than bpa due to the presence of one more −CH− group.

Crystal Structure of $[Zn(H_2pbta)(bibm)]\cdot H_2O$ (7). Compound **7** belongs to the $P\bar{1}$ space group, and its asymmetric unit contains one $[Zn(H_2pbta)(bibm)]$ unit and one water solvent molecule. The Zn(II) atom is tetrahedrally coordinated to two N atoms from bibm ligands and two O atoms from monodentate carboxylate groups of pbta (Figure 7a). Unlike the structures of **5** and **6**, two deprotonated carboxyl groups of H_2pbta^{2-} in **7** bind to two Zn(II) centers, while the other two keep protonated. In this way, each Zn(II) is connected to two H_2pbta^{2-} ligands to form a $[Zn_2(H_2pbta^{2-})_2]$ rectangle unit with a dimension of 12.3 Å × 10.9 Å. These units are pillared by bibm ligands to afford a 1D rectangle-shaped nanotube[68] (Figure 7b). Adjacent nanotubes are packed together through the hydrogen bonds and unconventional interactions (C−H···π, C−H···O). The whole architecture can be simplified as a 1D + 1D → 2D polycatenation motif when the Zn centers and the ligands are regarded as nodes and rods, respectively (Figure 7c,d). In this structure, each pbta works as a flexible ligand but bibm as a rigid one.

As described above, compounds **1**−**7** possesses quite different polydimensional architectures. These structural diversities are probably due to the rigidity versus flexibility of the ligands along with the number of carboxyl groups in carboxylate ligands. In **1**−**4**, the different conformations of the pbda ligand were observed though the same pbda was used. The structural diversities of **1**−**4** may also be ascribed to the rigidity or flexibility of the auxiliary N-donor ligands. Compound **2** displays a 2D + 2D + 2D → 2D interpenetrating network due to the flexible pbda. Pbda shows a flexible feature in **3** and **4**, while it exhibits a rigid character in **1**. When the number of carboxylate groups was increased to four, the employment of such a ligand (H_4pbta) led to the formation of different structures of **5**−**7**. As expected, it is hard for pbta to rotate its bulk groups freely to form the rods like motifs observed in **5**. Two carboxyl groups on one phenyl ring of pbta binded at Zn(II) simultaneously will restrict the movement of the ligand. Both phenyl rings (bonded by carboxyl groups) of pbta in **5** are nearly in a plane. Although **7** displays a rod-loop framework, each H_4pbta has its two carboxyl groups uncoordinated, which makes it act as H_2pbda in **1**−**4**. In addition, $[Zn_2(pbta)(bpa)_2]\cdot 4H_2O$[33] also shows that pbta binds the Zn ions by using two of its carboxyl groups, and the three benzene rings are nearly in a plane. **2** shows a similar motif to that of **7** with two adjacent rods penetrating into the loops formed by $Zn_2(pbda)_2$ units. However, **2** shows a 2D + 2D + 2D → 2D polycatenation network, while **7** displays a 1D + 1D → 2D network. Such a structural difference is probably due to the different positions of the carboxyl groups attached at the phenyl ring (*para*-position in **2**, and *meta*-position in **7**). The flexibility and the rigidity of the ligands interact with each other and which one dictates the final topologic structures of the resulting CPs highly depends on the lengths and geometries of the ligands employed.

Thermal Property. To characterize the thermal stability of these compounds, thermogravimetric analyses (TGA) of **1**−**7** (Figures S3 and S4) were carried out using a similar method.[10]

DOI: 10.1021/acs.cgd.5b00642
Cryst. Growth Des. XXXX, XXX, XXX−XXX

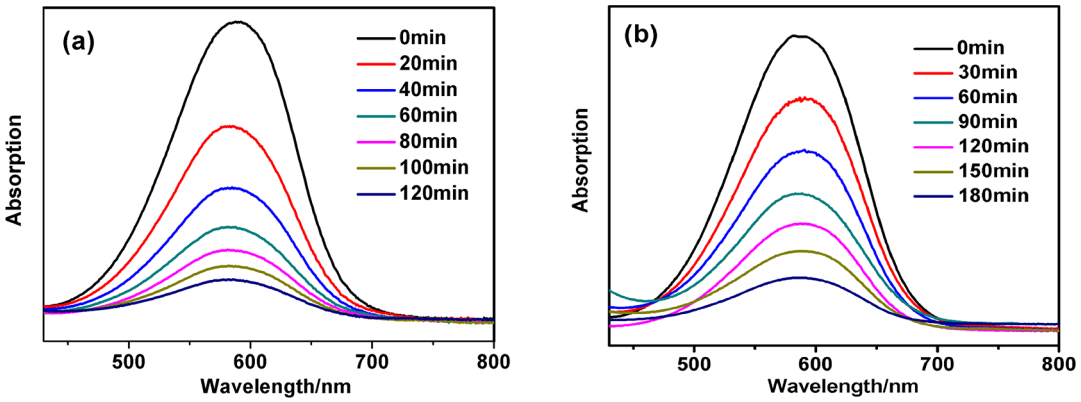

Figure 8. (a) Absorption spectra of the solutions of MB in the presence of **3** under sunlight irradiation. (b) Absorption spectra of the solutions of MB in the presence of **6** under sunlight irradiation.

The TGA analysis revealed that these compounds were quite stable up to 200 or 300 °C. Compound **1** lost 2.61% (calculated 2.59%) of its weight in the first stage from 25 to 200 °C, which can be assigned to the release of one lattice water molecule. After that, the structure began to collapse above 330 °C. Compound **2** was stable up to 370 °C and then decomposed into metal oxide at higher temperature. Compounds **3** and **4** showed high thermal stability below 300 °C. When the temperature was elevated, the products gradually lost pbda and p-bimb (**1**), bpa (**2**), bpp (**3**), or bibm (**4**). Compound **5** lost its lattice water molecule below 300 °C with the weight loss of 2.52% (calculated 3.25%). When the temperature increased, it began to decompose gradually. The weight loss between 30 and 150 °C of **6** can be assigned to dissociate of the coordinated water molecules (observed 2.65%; calculated 3.48%). For **7**, there was no weight loss observed in the range of 30−200 °C. The lattice water molecule may evaporate when samples are exposed to the air, and it started to decompose at 360 °C.

Photoluminescent Property. Coordination polymers with d^{10} metal centers[69−72] have been widely investigated for their photoluminescent properties and their potential applications as fluorescent materials.[73−75] In the present work, the photoluminescent properties of **1**−**7** together with the free H_2pbda and H_4pbta ligands were studied in the solid state at room temperature. The emission spectra of these compounds and the two carboxylate ligands were presented in Figures S5−S6. The free H_2pbda and H_4pbta ligands display intense emission bands with maxima about 340 and 358 nm (λ_{ex} = 280 nm), respectively, which may be attributed to the $\pi^* \rightarrow \pi$ transitions.[76−78] For **1**, the emission peak at 330 nm was found (λ_{ex} = 285 nm), which was similar to that of H_2pbda. Similarly, **6** and **7** showed the emission bands at about 358 and 356 nm, respectively, which are analogous to the H_4pbta ligand. The emissions of compounds **1**−**7** are tentatively ascribed to be a ligand-to-ligand charge transfer (LLCT) nature.[79−83] The emission bands at 440 and 354 nm (λ_{ex} = 290 nm) were observed for compounds **2** and **4**, which were highly red-shifted by 100 nm (**2**) and 14 nm (**4**) compared with the free H_2pbda. Compound **3** showed an intense emission band at ca. 309 nm (λ_{ex} = 290 nm), which was blue-shifted by 31 nm compared with the free H_2pbda. Compound **5** exhibited an intense emission band at 336 nm (λ_{ex} = 280 nm), which was blue-shifted by 22 nm compared with free H_4pbta (Figure 6). These emission origins may be assigned as either the ligand-to-metal charge transfer (LMCT) or LLCT transitions.[84−86] The different emission bands of **1**−**7** may be also ascribed to the rigidity versus flexibility of the ligands and their different architectures described above.[87]

Optical and Photocatalytic Properties. In order to investigate the optical properties of these compounds, compounds **3** and **6** were taken as representative examples. Following a similar method,[10] the band gap energies (E_{onset}) of **3** and **6** were estimated to be 3.4 and 3.6 eV, respectively (Figure S7). Thus, **3** and **6** may be regarded as semiconducting materials and employed as potential photocatalysts upon exposure to sunlight.[88−90]

The photocatalytic activities of **3** and **6** were assessed by decomposing MB in water under natural sunlight irradiation. As we know, the examples of the CPs exhibiting obvious photocatalytic properties for degrading MB under sunlight irradiation are very limited.[91] Herein, we examined the photocatalytic activities of **3** and **6** toward the decomposition of MB in water using sunlight irradiation. The typical procedures for the preparation of the MB solution and the catalyst were carried out according to the literature.[10] As shown in Figure 8, the absorption peaks of MB decreased obviously along with the increase of the reaction time. The photocatalytic activity increased from 25% (without any catalyst, Figure S8) to 87% for **3** and 83% for **6** after 180 min. Obviously, the degradation efficiency of **3** under sunlight irradiation was slightly higher than **6**, which may be attributed to the smaller energy gap of **3**.[92−97] Their efficiencies were somewhat higher than those obtained by coordination polymers under UV light irradiation reported recently.[98,99] For example, compounds $[Co(L_1)(1,3\text{-BDC})(H_2O)_2]$ (L_1 = *N*,*N*′-bis(3-pyridyl)-malonaminde) and $[Co(L_2)(L_3)_2]$ (H_4L_2 = tetrakis[4-(carboxyphenyl)-oxamethyl]methane acid, L_3 = 4-tolyl-2,2′:6′,2″-terpyridine) showed 81% and 46% degradation of MB after 130 and 210 min of UV light irradiation, respectively. The results showed that **3** and **6** possessed relatively high catalytic efficiencies for the degradation of MB in aqueous solution under sunlight. The PXRD patterns of the recycled samples (**3** and **6**) showed no obvious difference from those of as-synthesized **3** and **6** (Figure S9), indicating their good stability and recyclability in such photocatalytic degradation of organic dyes in water using natural sunlight irradiation.

CONCLUSIONS

In conclusion, seven entangled networks of **1**−**7** were isolated from solvothermal reactions of $ZnSO_4 \cdot 7H_2O$ with two poly(carboxylic acid) ligands (H_2pbda and H_4pbta) and five auxiliary N-donor ligands (p-bimb, bpa, bpp, m-bimb, and

DOI: 10.1021/acs.cgd.5b00642
Cryst. Growth Des. XXXX, XXX, XXX−XXX

Table 1. Crystal Data and Structure Refinement Parameters for 1−7

	1	2	3	4	5	6	7
empirical formula	$C_{36}H_{32}N_4O_7Zn$	$C_{28}H_{22}NO_6Zn$	$C_{35}H_{30}N_2O_6Zn$	$C_{80}H_{62}N_8O_{12}Zn$	$C_{26}H_{23}N_4O_6Zn$	$C_{25}H_{23}N_2O_6Zn$	$C_{42}H_{32}N_4O_{11}Zn$
formula weight	698.01	533.84	640.00	1392.75	552.84	512.82	834.09
crystal system	monoclinic	triclinic	triclinic	triclinic	monoclinic	triclinic	triclinic
space group	$P2_1/c$	$P\bar{1}$	$P\bar{1}$	$P\bar{1}$	$P2_1/c$	$P\bar{1}$	$P\bar{1}$
a (Å)	8.3471(17)	9.3717(19)	9.1199(18)	9.5318(19)	8.7037(17)	9.8901(8)	9.8893(9)
b (Å)	20.085(4)	11.209(2)	11.616(2)	12.490(3)	16.355(3)	11.001(7)	12.2772(11)
c (Å)	19.236(4)	12.227(2)	15.685(3)	14.214(3)	18.856(5)	11.9223(11)	15.8563(16)
α (deg)		109.67(3)	96.54(3)	76.45(3)		82.982(6)	75.014(8)
β (deg)	91.51(3)	96.74(3)	100.43(3)	86.68(3)	115.71(2)	77.657(7)	76.456(8)
γ (deg)		96.16(3)	106.40(3)	83.09(3)		65.772(7)	82.337(7)
V (Å^3)	3223.8(11)	1186.2(4)	1543.5(6))	1632.4(6)	2418.4(9)	1154.71(16)	1802.5(3)
Z	4	2	2	1	4	2	2
T/K	293(2)	296(2)	296(2)	293(2)	293(2)	293(2)	293(2)
D_{calcd} (g cm^{-3})	1.434	1.495	1.377	1.417	1.513	1.475	1.533
λ(Mo Kα) (Å)	0.71073	0.71073	0.71073	0.71073	0.71073	0.71073	0.71073
μ (mm^{-1})	0.819	1.081	0.844	0.451	1.066	1.108	0.754
F(000)	1440	550.0	664	724	1132	530	856
R_1[a]	0.0781	0.0415	0.0810	0.0953	0.0881	0.0325	0.0747
wR_2[b]	0.2025	0.0911	0.1424	0.2445	0.1749	0.0796	0.1769
GOF[c]	0.949	1.085	1.083	1.113	1.226	1.058	0.988

[a] $R_1 = \Sigma||F_0| - |F_c||/\Sigma|F_0|$. [b] $wR_2 = \{\Sigma w(F_0^2 - F_c^2)^2/\Sigma w(F_0^2)^2\}^{1/2}$. [c] GOF = $\{\Sigma w((F_0^2 - F_c^2)^2)/(n - p)\}^{1/2}$, where n = number of reflections and p = total numbers of parameters refined.

bibm). These compounds showed intriguing 1D, 2D, and 3D topological frameworks, which made them versatile candidates for the assembly of CPs with aesthetic structures. Their structural diversities demonstrate that the rigidity−flexibility relationship of the ligands along with the number of carboxyl groups exert significant impact on the self-assembly of coordination frameworks. The long flexible ligand which has only two carboxyl groups (H_2pbda) can easily form rod-like structures by bending its −O−CH_2− groups (**1**, **2**, and **7**). However, H_4pbta with two or more carboxyl groups on one phenyl ring coordinated to the metal can restrict the movement of some groups, which makes the ligand a rigid one (**5**). Under the sunlight irradiation, compounds **3** and **6** as representative examples exhibited high catalytic activity toward the photodegradation of MB in water. Both compounds show good stability and recyclability. These results further reveal that these compounds may become potential catalysts in photodecomposing some dye molecules in industrial wastewaters under visible light irradiation.

EXPERIMENTAL SECTION

General Procedures. The H_4pbta ligand was prepared according to a literature method.[46−50] The instruments involved in this article were the same as those used in our previous works unless otherwise noted.[10,21,25]

Synthesis. *H_2pbda.* H_2pbda was prepared according to a modified literature method.[46−50] A mixture of methyl 4-hydroxybenzoate (6.09 g, 40 mmol), α,α'-dibromo-*p*-xylene (5.28 g, 20 mmol), 18-crown-6 (0.13 g, 0.5 mmol), and K_2CO_3 (6.08 g, 44 mmol) in acetone (100 mL) was refluxed for 20 h. The mixture was then cooled to ambient temperature and CH_2Cl_2 (60 mL) was added. After the resulting mixture was further stirred for 30 min and filtered, the filtrate was concentrated to dryness *in vacuo*, and the residue was dissolved in CH_3OH (200 mL) at 70 °C. H_2O (100 mL) was then added and cooled to room temperature again. The resulting solid was collected, washed with CH_3OH/H_2O (v/v = 2:1), and dried at 80 °C for 10h to obtain 7.56 g (93%) of ester H_2pbda as a white solid. To a solution of ester H_2pbda (1.624 g, 4.0 mmol) was added KOH (1.120 g, 20 mmol), methanol (30 mL), and water (30 mL). The resulting mixture was stirred under nitrogen at 80 °C for 12 h and then concentrated *in vacuo*. A 3 M HCl aqueous solution was added slowly into the solution at room temperature to afford a white solid, which was collected, washed with water, and dried *in vacuo* to give 1.38 g (85%) of H_2pbda. IR (KBr, cm^{-1}): 3075 (w), 3012 (w), 2953 (m), 2892 (w), 1673 (vs), 1603 (s), 1502 (s), 1427 (s), 1372 (s), 1253 (s), 1162 (s), 1102 (m), 1032 (m), 1012 (w), 953 (w), 842 (s), 773 (s), 643 (s). ^{1}H NMR (DMSO-d_6, δ): 5.201 (4H, s), 7.114 (4H, d), 7.496 (4H, d), 7.907 (4H, d) (Figure S10).

*[Zn(pbda)(p-bimb)]·H_2O (**1**).* A mixture containing $ZnSO_4{\cdot}7H_2O$ (29 mg, 0.1 mmol), H_2pbda (19 mg, 0.05 mmol), p-bimb (12 mg, 0.05 mmol), and 2 mL of H_2O and DMF (v/v = 6:4) was loaded in a thick Pyrex tube. The tube was then sealed and heated to 145 °C for 2 days. After that, it was cooled to ambient temperature at a rate of 5 °C/h to afford colorless crystals of **1** in 51% yield (based on $ZnSO_4{\cdot}7H_2O$). Anal. Calcd for $C_{36}H_{32}N_4O_7Zn$: C, 61.94; H, 4.58; N, 8.02%. Found: C, 62.02; H, 4.65; N, 7.91%. IR (KBr disk, cm^{-1}): 3436 (w), 1602 (m), 1248 (m), 1101 (w), 1061 (w), 851 (w), 782 (m), 654 (s).

*[Zn(pbda)(bpa)$_{0.5}$] (**2**).* Compound **2** was obtained as colorless block crystals by using a similar method to that described for **1**, except that p-bimb was replaced by bpa (9.4 mg, 0.05 mmol). Yield: 60% (based on $ZnSO_4{\cdot}7H_2O$). Anal. Calcd for $C_{28}H_{22}NO_6Zn$: C, 62.99; H, 4.12; N, 2.62%. Found: C, 62.92; H, 4.23; N, 2.50%. IR (KBr disk, cm^{-1}): 1634 (s), 1602 (m), 1540 (m), 1394 (s), 1251 (m), 1174 (m), 1105 (w), 853 (w), 782 (m), 648 (s).

*[Zn(pbda)(bpp)] (**3**).* Compound **3** was prepared in an route analogous to that used for the isolation of **1**, with $ZnSO_4{\cdot}7H_2O$ (29 mg, 0.1 mmol), H_2pbda (19 mg, 0.05 mmol), bpp (10 mg, 0.05 mmol), and 2 mL of H_2O and DMF (v/v = 6:4). Yield: 40% (based on $ZnSO_4{\cdot}7H_2O$). Anal. Calcd for $C_{35}H_{30}N_2O_6Zn$: C, 65.68; H, 4.69; N, 4.38%. Found: C, 65.60; H, 4.72; N, 4.45%. IR (KBr disk, cm^{-1}): 1601 (m), 1540 (m), 1396 (w), 1251 (m), 1101 (w), 846 (m), 782 (m), 659 (s).

*[Zn(Hpbda)$_2$(bibm)$_2$] (**4**).* Compound **4** was prepared in a similar method to that used for the isolation of **1**, except that p-bimb was replaced by bibm (14 mg, 0.05 mmol). Yield: 45% (based on $ZnSO_4{\cdot}7H_2O$). Anal. Calcd for $C_{80}H_{62}N_8O_{12}Zn$: C, 68.99; H, 4.45; N, 8.04%. Found: C, 69.10; H, 4.43; N, 7.92%. IR (KBr disk, cm^{-1}): 1602 (s), 1571 (s), 1456 (s), 1303 (s), 1247 (s), 1170 (m), 1058 (w), 846 (m), 785 (m), 659 (w), 534 (m).

DOI: 10.1021/acs.cgd.5b00642
Cryst. Growth Des. XXXX, XXX, XXX−XXX

[Zn(pbta)$_{0.5}$(m-bimb)]·H$_2$O (**5**). Compound **5** was prepared as colorless block crystals by the same synthetic procedure for **1**, from $ZnSO_4·7H_2O$ (29 mg, 0.1 mmol), H_4pbta (23 mg, 0.05 mmol), m-bimb (12 mg, 0.05 mmol), and 2 mL of H_2O and DMF (v/v = 6:4). Yield: 50% (based on $ZnSO_4·7H_2O$). Anal. Calcd for $C_{26}H_{23}N_4O_6Zn$: C, 56.48; H, 4.16; N, 10.13%. Found: C, 56.50; H, 4.19; N, 10.21%. IR (KBr disk, cm^{-1}): 3444 (m), 1623 (s), 1607 (m), 1576 (m), 1489 (m), 1452 (m), 1371 (s), 1266 (m), 1093 (m), 1036 (s), 853 (w), 776 (s), 658 (m).

[Zn(pbta)$_{0.5}$(bpp)(H$_2$O)] (**6**). Compound **6** was prepared as colorless block crystals by the same synthetic procedure for **1**, from $ZnSO_4·7H_2O$ (29 mg, 0.1 mmol), H_4pbta (22 mg, 0.05 mmol), bpp (11 mg, 0.05 mmol), and 2 mL of H_2O/DMF (v/v = 6:4). Yield: 60% (based on $ZnSO_4·7H_2O$). Anal. Calcd for $C_{25}H_{23}N_2O_6Zn$: C, 58.55; H, 4.48; N, 5.46%. Found: C, 58.60; H, 4.40; N, 5.50%. IR (KBr disk, cm^{-1}): 3292 (m), 1622 (s), 1577 (s), 1505 (m), 1452 (m), 1396 (m), 1366 (m), 1266 (w), 1236 (m), 1123 (m), 1097 (m), 1037 (m), 778 (s), 728 (m), 640 (m), 517 (m).

[Zn(H$_2$pbta)(bibm)]·H$_2$O (**7**). Compound **7** was prepared as colorless sheet crystals by the same synthetic procedure for **1** was used, from $ZnSO_4·7H_2O$ (29 mg, 0.1 mmol), bibm (14 mg, 0.05 mmol), H_4pbta (24 mg, 0.05 mmol), and 2 mL of H_2O and DMF (v/v = 6:4). Yield: 48% (based on $ZnSO_4·7H_2O$). Anal. Calcd for $C_{42}H_{32}N_4O_{11}Zn$: C, 60.47; H, 3.83; N, 6.71%. Found: C, 60.56; H, 3.96; N, 6.82%. IR (KBr disk, cm^{-1}): 3474 (m), 1706 (s), 1621 (s), 1571 (s), 1521 (s), 1452 (m), 1395 (m), 1310 (m), 1259 (m), 1125 (m), 1065 (m), 1041 (m), 1036 (m), 964 (m), 824 (m), 778 (s), 729 (m), 657 (m).

X-ray Structure Determinations. Crystal data for **1**−**7** were collected on a Bruker ApexII smart using graphite monochromated Mo−Kα (λ = 0.71073 Å). The collected data were reduced by the program ApexII. The crystal structures of **1**−**7** were solved by direct methods and refined on F^2 by full-matrix least-squares methods with the *SHELXL*-97 program.[100] All non-hydrogen atoms were refined anisotropically. The H (H5a) atom of the protonated carboxyl group in **5** was located in the different maps. The H atoms of the lattice water molecules in **1**, **5**, and **7** were not located in the different Fourier maps but were added to their formula. Crystallographic data and refinement details for **1**−**7** are summarized in Table 1.

■ ASSOCIATED CONTENT

Ⓢ Supporting Information

Crystal structural data for **1**−**7** (CCDC 1007803−100787, 100789, and 1007810) in CIF, additional figures and details of characterization (pdf). The Supporting Information is available free of charge on the ACS Publications website at DOI: 10.1021/acs.cgd.5b00642.

■ AUTHOR INFORMATION

Corresponding Authors

*(J.-P.L.) Tel./Fax: +86 512 65880328; e-mail: jplang@suda.edu.cn.

*(Q.H.) Tel./Fax: +86 771 3267118; e-mail: huangqinpeking@163.com.

Author Contributions

#S.L.W. and F.-L.H. contributed equally to this work

Notes

The authors declare no competing financial interest.

■ ACKNOWLEDGMENTS

The authors acknowledge the financial support from the National Natural Science Foundation of China (21463006, 21171124, 21373142 and 51203027). J.-P.L. highly appreciates the financial support from the Qing-Lan Project and the "333" Project of Jiangsu Province, the Priority Academic Program Development of Jiangsu Higher Education Institutions, and the "SooChow Scholar" Program of Soochow University. F.-L.H. also acknowledges the financial support from the Innovative Research Program for Postgraduates in Universities of Jiangsu Province (KYZZ-0335) and the Guangxi Natural Science Foundation (2014GXNSFBA118044). The authors are grateful for the useful comments and suggestions of the editors and reviewers.

■ REFERENCES

(1) Hagrman, P.; Hagrman, D.; Zubieta, J. *Angew. Chem., Int. Ed.* **1999**, *111*, 2798−2848.
(2) Yao, Z. J.; Yu, W. B.; Huang, S. L.; Li, Z. H.; Jin, G. X. *J. Am. Chem. Soc.* **2014**, *136*, 2825−2832.
(3) Huang, S. L.; Lin, Y. J.; Andy Hor, T. S.; Jin, G. X. *J. Am. Chem. Soc.* **2013**, *135*, 8125−8128.
(4) Blake, A.; Champness, N.; Hubberstey, P.; Li, W.; Withersby, M.; Schröder, M. *Coord. Chem. Rev.* **1999**, *183*, 117−138.
(5) Moulton, B.; Zaworotko, M. *Chem. Rev.* **2001**, *101*, 1629−1658.
(6) Evans, O.; Lin, W. B. *Acc. Chem. Res.* **2002**, *35*, 511−522.
(7) Yaghi, M.; OKeeffe, M.; Ockwig, N.; Chae, H.; Eddaoudi, M.; Kim, J. *Nature* **2003**, *423*, 705−714.
(8) Müller, A.; Das, S.; Talismanov, S.; Roy, S.; Beckmann, E.; Bögge, H.; Schmidtmann, M.; Merca, A.; Berkle, A.; Allouche, L.; Zhou, Y.; Zhang, L. *Angew. Chem., Int. Ed.* **2003**, *115*, 5193−5198.
(9) Rao, C.; Natarajan, S.; Vaidhyanathan, R. *Angew. Chem., Int. Ed.* **2004**, *116*, 1490−1521.
(10) Hu, F. L.; Wang, S. L.; Wu, B.; Yu, H.; Wang, F.; Lang, J. P. *CrystEngComm* **2014**, *16*, 6354−6363.
(11) Béziau, A.; Baudron, S. A.; Pogozhev, D.; Fluck, A.; Hosseini, M. W. *Chem. Commun.* **2012**, *48*, 10313−10315.
(12) Chen, X. Y.; Marchal, C.; Filinchuk, Y.; Imbert, D.; Mazzanti, M. *Chem. Commun.* **2008**, 3378−3380.
(13) Bu, X. H.; Chen, W.; Hou, W. F.; Du, M.; Zhang, R. H.; Brisse, F. *Inorg. Chem.* **2002**, *41*, 3477−3482.
(14) Liu, Y. Y.; Ma, J. F.; Yang, J.; Su, Z. M. *Inorg. Chem.* **2007**, *46*, 3027−3037.
(15) Zhang, L. P.; Ma, J. F.; Yang, J.; Liu, Y. Y.; Wei, G. H. *Cryst. Growth Des.* **2009**, *9*, 4660−4673.
(16) Suenaga, Y.; Yan, S. G.; Wu, L. P.; Ion, I.; Kuroda-Sowa, T.; Maekawa, M.; Munakata, M. J. *Chem. Soc., Dalton Trans.* **1998**, 1121−1126.
(17) Hirsch, K. A.; Wilson, S. R.; Moore, J. S. *Inorg. Chem.* **1997**, *36*, 2960−2968.
(18) Bu, X. H.; Xie, Y. B.; Li, J. R.; Zhang, R. *Inorg. Chem.* **2003**, *42*, 7422−7430.
(19) Knight, J. C.; Alvarez, S.; Amoroso, A. J.; Edwards, P. G.; Singh, N. *Dalton Trans.* **2010**, *39*, 3870−3883.
(20) Zhang, X.; Guo, C.; Yang, Q.; Wang, W.; Liu, W.; Kang, B.; Su, C. *Chem. Commun.* **2007**, 4242−4244.
(21) Hu, F. L.; Wu, W.; Liang, P.; Gu, Y. Q.; Zhu, L. G.; Wei, H.; Lang, J. P. *Cryst. Growth Des.* **2013**, *13*, 5050−5061.
(22) Qin, C.; Wang, X.; Carlucci, L.; Tong, M.; Wang, E.; Hu, C.; Xu, L. *Chem. Commun.* **2004**, 1876−1877.
(23) Du, M.; Wang, X. G.; Zhang, Z. H.; Tang, L. F.; Zhao, X. J. *CrystEngComm* **2006**, *8*, 788−793.
(24) Liu, D.; Ren, Z. G.; Li, H. X.; Lang, J. P.; Li, N. Y.; Abrahams, B. F. *Angew. Chem., Int. Ed.* **2010**, *49*, 4767−4770.
(25) Hu, F. L.; Wang, S. L.; Lang, J. P.; Abrahams, B. F. *Sci. Reports* **2014**, *4*, 6815−6820.
(26) Liu, D.; Lang, J. P. *CrystEngComm* **2014**, *16*, 76−81.
(27) Blake, A.; Champness, N.; Khlobystov, A.; Lemenovskii, D.; Li, W.; Schröder, M. *Chem. Commun.* **1997**, 2027−2028.
(28) Yang, J.; Ma, J.; Batten, S.; Su, Z. *Chem. Commun.* **2008**, 2233−2235.
(29) Yao, Q.; Ju, Z.; Zhang, J. *Inorg. Chem.* **2009**, *48*, 1266−1268.
(30) He, X.; Lu, X. P.; Li, M. X.; Morris, R. E. *Cryst. Growth Des.* **2013**, *13*, 1649−1654.

DOI: 10.1021/acs.cgd.5b00642
Cryst. Growth Des. XXXX, XXX, XXX−XXX

(31) He, X.; Lu, X. P.; Ju, Z. F.; Li, C. J.; Zhang, Q. K.; Li, M. X. *CrystEngComm* **2013**, *15*, 2731−2734.
(32) Sun, D.; Han, L. L.; Yuan, S.; Deng, Y. K.; Xu, M. Z.; Sun, D. F. *Cryst. Growth Des.* **2013**, *13*, 377−385.
(33) Parshamoni, S.; Sanda, S.; Jena, H. M.; Tomar, K.; Konar, S. *Cryst. Growth Des.* **2014**, *14*, 2022−2033.
(34) Du, M.; Jiang, X. J.; Zhao, X. J. *Inorg. Chem.* **2006**, *45*, 3998−4006.
(35) Martin, D. P.; Staples, R. J.; LaDuca, R. L. *Inorg. Chem.* **2008**, *47*, 9754−9756.
(36) LaDuca, R. L. *Coord. Chem. Rev.* **2009**, *253*, 1759−1792.
(37) Yao, X. Q.; Cao, D. P.; Hu, J. S.; Li, Y. Z.; Guo, Z. J.; Zheng, H. G. *Cryst. Growth Des.* **2011**, *11*, 231−239.
(38) Li, B.; Zang, S. Q.; Ji, C.; Du, C. X.; Hou, H. W.; Mak, T. C. W. *Dalton Trans.* **2011**, *40*, 788−792.
(39) Fang, S. M.; Hu, M.; Zhang, Q.; Du, M.; Liu, C. S. *Dalton Trans.* **2011**, *40*, 4527−4541.
(40) Gu, J. Z.; Gao, Z. Q.; Tang, Y. *Cryst. Growth Des.* **2012**, *12*, 3312−3323.
(41) Su, Z.; Fan, J.; Chen, M.; Okamura, T.; Sun, W. Y. *Cryst. Growth Des.* **2011**, *11*, 1159−1169.
(42) Shi, D. B.; Ren, Y. W.; Jiang, H. F.; Cai, B. W.; Lu, J. X. *Inorg. Chem.* **2012**, *51*, 6498−6506.
(43) Ma, L. F.; Wang, L. Y.; Wang, Y. Y.; Batten, S. R.; Wang, J. G. *Inorg. Chem.* **2009**, *48*, 915−924.
(44) Ma, L. F.; Li, C. P.; Wang, L. Y.; Du, M. *Cryst. Growth Des.* **2011**, *11*, 3309−3312.
(45) Liu, T. F.; Lu, J. A.; Tian, C. B.; Cao, M. N.; Lin, Z. J.; Cao, R. *Inorg. Chem.* **2011**, *50*, 2264−2271.
(46) Schaate, A.; Klingelhofer, S.; Behrens, V.; Wiebcke, M. *Cryst. Growth Des.* **2008**, *8*, 3200−3205.
(47) Liu, Y.; Qi, Y.; Lv, Y. Y.; Che, Y. X.; Zheng, J. M. *Cryst. Growth Des.* **2009**, *9*, 4797−4801.
(48) Li, Z. X.; Hu, T. L.; Ma, H.; Zeng, Y. F.; Li, C. J.; Tong, M. L.; Bu, X. H. *Cryst. Growth Des.* **2010**, *10*, 1138−1144.
(49) Yang, J.; Ma, J. F.; Battern, S. R.; Su, Z. M. *Chem. Commun.* **2008**, 2221−2223.
(50) Pachfule, P.; Dey, C.; Panda, T.; Banarjee, R. *CrystEngComm* **2010**, *12*, 1600−1609.
(51) Cao, X. Y.; Yao, Y. G.; Batten, S. R.; Ma, E.; Qin, Y. Y.; Zhang, J.; Zhang, R. B.; Cheng, J. K. *CrystEngComm* **2009**, *11*, 1030−1036.
(52) Pan, Y. J.; Ford, W. T. *J. Org. Chem.* **1999**, *64*, 8588−8593.
(53) Kalsi, P. S. *Spectroscopy Of Organic Compounds*; New Age International: New Delhi. 2008.
(54) Ma, T.; Li, M. X.; Wang, Z. X.; Zhang, J. C.; Shao, M.; He, X. *Cryst. Growth Des.* **2014**, *14*, 4155−4165.
(55) Bellamy, L. J. *The Infrared Spectra of Compound Molecules*; Wiley: New York. 1958.
(56) Zhang, F. M.; Zou, X. Y.; Yan, P. F.; Li, G. M. *Cryst. Growth Des.* **2015**, *15*, 1249−1258.
(57) Arıcı, M.; Yeşilel, O. Z.; Taş, M. *Cryst. Growth Des.* **2015**, *15*, 3024−3031.
(58) Du, P.; Yang, Y.; Yang, J.; Liu, Y. Y.; Ma, J. F. *CrystEngComm* **2013**, *15*, 6986−7002.
(59) Ji, C. C.; Qin, L.; Li, Y. Z.; Guo, Z. J.; Zheng, H. G. *Cryst. Growth Des.* **2011**, *11*, 480−487.
(60) Batten, S. R.; Robson, R. *Angew. Chem., Int. Ed.* **1998**, *37*, 1460−1494.
(61) Batten, S. R. *CrystEngComm* **2001**, *3*, 67−72.
(62) Carlucci, L.; Ciani, G.; Proserpio, D. M. *Coord. Chem. Rev.* **2003**, *246*, 247−289.
(63) Goodgame, D. M. L.; Menzer, S.; Smith, A. M.; Williams, D. J. *Angew. Chem., Int. Ed.* **1995**, *34*, 574−575.
(64) Luo, F.; Yang, Y. T.; Che, Y. X.; Zheng, J. M. *CrystEngComm* **2008**, *10*, 981−982.
(65) Lan, Y. Q.; Li, S. L.; Qin, J. S.; Du, D. Y.; Wang, X. L.; Su, Z. M.; Fu, Q. *Inorg. Chem.* **2008**, *47*, 10600−10610.
(66) Yang, Q. X.; Chen, X. Q.; Cui, J. H.; Hu, J. S.; Zhang, M. D.; Qin, L.; Wang, G. F.; Lu, Q. Y.; Zheng, H. G. *Cryst. Growth Des.* **2012**, *12*, 4072−4082.
(67) Xu, L.; Guo, G. C.; Liu, B.; Wang, M. S.; Huang, J. S. *Inorg. Chem. Commun.* **2004**, *7*, 1145−1149.
(68) Chen, S. M.; Zhang, J. A.; Lu, C. Z. *CrystEngComm* **2007**, *9*, 390−393.
(69) Valeur, B. *Molecular Fluorescence: Principles and Application*; Wiley-VCH: Weinheim, 2002.
(70) Zheng, S. L.; Yang, J. H.; Yu, X. L.; Chen, X. M.; Wang, W. T. *Inorg. Chem.* **2004**, *43*, 830−838.
(71) He, J. H.; Yu, J. H.; Zhang, Y. T.; Pan, Q. H.; Xu, R. R. *Inorg. Chem.* **2005**, *44*, 9279−9282.
(72) Liang, X. Q.; Zhou, X. H.; Chen, C.; Xiao, H. P.; Li, Y. Z.; Zou, J. L.; You, X. Z. *Cryst. Growth Des.* **2009**, *9*, 1041−1053.
(73) Bunz, U. H. F. *Chem. Rev.* **2000**, *100*, 1605−1644.
(74) Frisch, M.; Cahill, C. L. *Dalton Trans.* **2005**, *8*, 1518−1523.
(75) Yu, G.; Yin, S.; Liu, Y.; Shuai, Z.; Zhu, D. *J. Am. Chem. Soc.* **2003**, *125*, 14816−14824.
(76) Chen, S. S.; Zhao, Y.; Fan, J.; Okamura, T.; Bai, Z. S.; Chen, Z. H.; Sun, W. Y. *CrystEngComm* **2012**, *14*, 3564−3576.
(77) Xu, C. Y.; Li, L. K.; Wang, Y. P.; Guo, Q. Q.; Wang, X. J.; Hou, H. W.; Fan, Y. T. *Cryst. Growth Des.* **2011**, *11*, 4667−4675.
(78) Cheng, P. C.; Kuo, P. T.; Liao, Y. H.; Xie, M. Y.; Hsu, W.; Chen, J. D. *Cryst. Growth Des.* **2013**, *13*, 623−632.
(79) Gong, Y.; Wu, T.; Lin, J. H.; Wang, B. S. *CrystEngComm* **2012**, *14*, 5649−5656.
(80) Bai, Y.; He, G. J.; Zhao, Y. G.; Duan, C. Y.; Dang, D. B.; Meng, Q. J. *Chem. Commun.* **2006**, 1530−1532.
(81) Zou, J. P.; Peng, Q.; Wen, Z.; Zeng, G. S.; Xing, Q. J.; Guo, G. C. *Cryst. Growth Des.* **2010**, *10*, 2613−2619.
(82) Wang, X. L.; Luan, J.; Sui, F. F.; Lin, H. Y.; Liu, G. C.; Xu, C. *Cryst. Growth Des.* **2013**, *13*, 3561−3576.
(83) Barbieri, A.; Accorsi, G.; Armaroli, N. *Chem. Commun.* **2008**, 2185−2193.
(84) Yang, G. P.; Wang, Y. Y.; Zhang, W. H.; Fu, A. Y.; Liu, R. T.; Lermontova, E. K.; Shi, Q. Z. *CrystEngComm* **2010**, *12*, 1509−1517.
(85) Chang, Z.; Zhang, A. S.; Hu, T. L.; Bu, X. H. *Cryst. Growth Des.* **2009**, *9*, 4840−4846.
(86) Wang, H. Y.; Gao, S.; Huo, L. H.; Ng, S. W.; Zhao, J. G. *Cryst. Growth Des.* **2008**, *8*, 665−670.
(87) Gong, Y.; Wua, T.; Lin, J. H. *CrystEngComm* **2012**, *14*, 3727−3736.
(88) Paul, A. K.; Madras, G.; Natarajan, S. *Phys. Chem.* **2009**, *11*, 11285−11296.
(89) Yang, G. S.; Zang, H. Y.; Lan, Y. Q.; Wang, X. L.; Jiang, C. J.; Su, Z. M.; Zhu, L. D. *CrystEngComm.* **2011**, *13*, 1461−1466.
(90) Tzeng, B. C.; Chiu, T. H.; Chen, B. S.; Lee, G. H. *Chem.—Eur. J.* **2008**, *14*, 5237−5245.
(91) Luo, F.; Yuan, Z. Z.; Feng, X. F.; Batten, S. R.; Li, J. Q.; Luo, M. B.; Liu, S. J.; Xu, W. Y.; Sun, G. M.; Song, Y. M.; Huang, H. X.; Tian, X. Z. *Cryst. Growth Des.* **2012**, *12*, 3392−3396.
(92) Liu, B.; Yang, J.; Yang, G. C.; Ma, J. F. *Inorg. Chem.* **2013**, *52*, 84−94.
(93) Wang, F.; Li, F. L.; Xu, M. M.; Yu, H.; Zhang, J. G.; Xia, H. T.; Lang, J. P. *J. Mater. Chem. A* **2015**, *3*, 5908−5916.
(94) Dai, M.; Su, X. R.; Wang, X.; Wu, B.; Ren, Z. G.; Zhou, X.; Lang, J. P. *Cryst. Growth Des.* **2014**, *14*, 240−248.
(95) Li, D. X.; Ni, C. Y.; Chen, M. M.; Dai, M.; Zhang, W. H.; Yan, W. Y.; Qi, H. X.; Ren, Z. G.; Lang, J. P. *CrystEngComm* **2014**, *16*, 2158−2167.
(96) Wen, T.; Zhang, D. X.; Zhang, J. *Inorg. Chem.* **2013**, *52*, 12−14.
(97) Kan, W. Q.; Liu, B.; Yang, J.; Liu, Y. Y.; Ma, J. F. *Cryst. Growth Des.* **2012**, *12*, 2288−2298.
(98) Guo, J.; Ma, J. F.; Li, J. J.; Yang, J.; Xing, S. X. *Cryst. Growth Des.* **2012**, *12*, 6074−6082.
(99) Wang, X. L.; Sui, F. F.; Lin, H. Y.; Zhang, J. W. *Cryst. Growth Des.* **2014**, *14*, 3438−3452.

DOI: 10.1021/acs.cgd.5b00642
Cryst. Growth Des. XXXX, XXX, XXX−XXX

(100) Sheldrick, G. M. *SHELXS-97, Program for Solution of Crystal Structures*; University of Göttingen: Germany, 1997.

DOI: 10.1021/acs.cgd.5b00642
Cryst. Growth Des. XXXX, XXX, XXX−XXX